Spectro-thermodynamics and molecular docking analysis of abiraterone and its binding to calf thymus DNA

Tanveer A. Wani*[1], Ahmed H. Bakheit[1,3], Abdurrahman A. Al-Mehizia[1], Azmat Ali Khan[1], Seema Zargar[2]

1. Department of Pharmaceutical Chemistry, College of Pharmacy, King Saud University, P.O. Box 2457, Riyadh 11451, Saudi Arabia
2. Department of Biochemistry, College of Science, King Saud University, PO Box 22452, Riyadh 11451, Saudi Arabia
3. Department of Chemistry, Faculty of Science and Technology, Al-Neelain University, Khartoum, Sudan.

*Corresponding author:

Dr. Seema Zargar

Department of Biochemistry, College of Science, King Saud University

Riyadh 11451, Saudi Arabia.

E-mail: szargar@ksu.edu.sa

Abstract

Binding of toxic ligands to DNA could result in undesirable biological processes, such as carcinogenesis or mutagenesis. Binding mode of abiraterone, a steroid drug and CT-DNA (calf thymus DNA was investigated in this study using fluorescence and ultraviolet–visible spectroscopy. The probable prediction of binding and the type of interaction forces involved in the arrangement between abiraterone and CT-DNA were explored through spectroscopic and molecular docking studies. The results indicated the binding of abiraterone to CT-DNA in the minor groove. The binding constants were in the range of $1.35 \times 10^6 – 0.36\times 10^6$ L mol^{-1} at the studied temperatures. Fluorescence and spectrophotometric data suggested static quenching between CT-DNA and abiraterone The endothermic values of thermodynamic parameters ΔH = -82.8 kJ mol^{-1}; ΔS = -161 J mol^{-1} K^{-1} suggested that hydrogen bondinging is the main force involved in binding CT-DNA and abiraterone. In experimental studies the free binding energy at 298K was −34.9 kJ mol^{-1} with the relative binding energy ≈ −29.65 kJ mol^{-1} of docked structure. The Ksv obtained for abiraterone-KI was similar to that for abiraterone-CT-DNA-KI demonstrating no protection by CT-DNA against quenching effect of KI. Thus, suggesting involvement of groove binding between abiraterone and CT-DNA. No change in the fluorescence intensity of abiraterone-CT-DNA was observed in presence of NaCl. Thus, ruling out the involvement of electrostatic interaction.These studies could serve as new insights in understanding the mechanisms of toxicity, resistance and side effects of abiraterone.

Keywords: abiraterone; DNA; binding; fluorescence; quenching, docking

Introduction

Interaction studies of biological macromolecules with drugs are important to comprehend the mechanism involved in their interaction [1]. Abiraterone is a pregnenolone derivative (3β)-17-(pyridin-3-yl) androsta-5,16-dien-3-ol steroid (Figure 1). Abiraterone was developed by Institute of Cancer Research, United Kingdom. Abiraterone is used in treatment of metastatic castration-resistant prostate cancer [2-4]. The reduced testosterone levels of <50 ng/dl have been observed after treatment with abiraterone in prostate cancer [5-7].

The interaction of drugs with CT-DNA *in-vitro* using spectroscopic methods is currently a growing interest in research to elucidate their mechanism of action [8-11]. In general, a double stranded CT-DNA could bind to the drug molecules by direct intercalation or groove binding or electrostatic interaction [8, 9]. Drugs that are capable of binding to DNA can alter the vital functions of cells by altering the expression and/or interfere in functioning of drug itself by causing drug resistance. Reactive oxygen species may also get generated because of these interactions in the DNA vicinity leading to its damage [8, 12]. Hence, the DNA- drug binding studies are valuable to understand the binding action mechanisms to DNA [13, 14]. CT-DNA is preferred in these studies because of its ease in availability, structural similarities with mammalian DNA and cost effectiveness.

This study was undertaken to explore the molecular mechanisms of interaction of abiraterone with CT-DNA and the effect of this interaction on the CT-DNA itself. UV–vis absorption and fluorescence spectroscopy studies along with molecular docking analysis were performed. Further, thermodynamic studies, evaluation of quenching and binding constants, displacement studies, potassium iodide quenching studies and ionic strength studies were carried out in order

to evaluate the interaction mechanism. The experimental results were corroborated with the results from molecular docking.

Materials

Abiraterone, CT-DNA and Ethidium bromide were purchased from Sigma Aldrich USA. Tris-HCl was procured from Himedia, India. Other reagents and chemicals used had analytical grade purity.

Sample preparation

Abiraterone stock solution (10mM) in ethanol and CT-DNA stock (10 mg per 10 mL) in Tris-HCl 10 mM (pH 7.4) stock were prepared. The CT-DNA solution was kept overnight at 4°C with intermittent shaking to make a homogenous solution. The concentration of CT-DNA stock was determined with UV absorbance spectrophotometer at 260nm using molar absorption coefficient of 6600M^{-1} cm^{-1}. The CT-DNA purity was calculated from the A260/A280 ratio, and ratio of 1.887 indicated a protein free CT-DNA. The prepared stocks were stored in dark at 4°C.

Methods

UV–vis spectroscopy

The UV–visible absorption spectra were acquired with Shimadzu spectrophotometer (model UV-1800, Japan). The absorption spectra (200-400 nm) for abiraterone and abiraterone bound CT-DNA complex were recorded. The concentration of abiraterone was fixed (50 μM) with the changing concentration of CT-DNA that ranged between 0–50 μM.

Fluorescence spectroscopy-based experiments

The fluorescence spectra for abiraterone□CT-DNA interaction were acquired with JASCO-8200 spectrofluorometer. The emission spectra of abiraterone (50μM) were recorded and studied in presence of CT-DNA (0□50μM). The excitation wavelength (λ_{ex}=265 nm) and emission wavelength (λ_{em}=280-335 nm) were used to record the fluorescence spectra at (298, 303, and 310 K). Tris□HCl buffer was used to prepare the samples and the measurements were carried out in using 1.0□cm quartz cells.

Iodide quenching studies

Iodide studies were conducted to determine the binding mode between abiraterone and CT-DNA. Potassium iodide (KI) solutions ranging between (0-80 μm) were interacted with abiraterone and abiraterone–CT-DNA separately and fluorescence intensities were recorded. Comparison of calculated Stern-Volmer constant (K_{sv}) of the KI with abiraterone and KI with abiraterone- CT-DNA helped in establishing the binding mode between abiraterone and CT-DNA

Ionic strength studies

The fluorescence emission spectra for abiraterone and abiraterone CT-DNA were recorded in presence of sodium chloride (NaCl). Different NaCl concentrations varying from 0- 70 μM were used while as, the concentrations of abiraterone and CT-DNA were fixed.

Molecular docking

Protein Data Bank (http://www.rcsb.org/pdb) was used to download the DNA structure (PDB ID-1BNA). For the docking analysis Molecular Operating Environment (MOE) was used and abiraterone structure was drawn within MOE. Default parameters MMFF94X for field force to attain energy minimization and default triangular matcher was used. London dG and GBVI/WSA

dG were the scoring functions 1 and 2, respectively. The root mean square values were evaluated to find the most suitable interaction.

Results and Discussion

UV-visible absorption spectral studies

The absorption spectra of abiraterone with CT-DNA are given in Figure 2. It was observed that with increasing concentration of CT-DNA there was increase in the absorbance with a blue shift of 10 nm. Previous studies reported that the ligand interaction with DNA can lead to formation of complex, and the formed complex might cause red or blue shift in the absorbance of the system [9, 15]. Since an increase in the absorbance was observed, hence, intercalative binding between CT-DNA and abiraterone is ruled out and minor groove binding between abiraterone and CT-DNA is suggested. These findings are concomitant to previous studies of CT-DNA with other drugs [16-18].

Analysis on the interaction mechanism

Fluorescence spectrum

The mechanism of interaction between ligands and bio-macromolecules can be understood using steady state fluorescence spectroscopy. The fluorescence spectroscopy helps in computing the binding constant and provides information regarding the type of forces involved in the interaction. Abiraterone demonstrated fluorescence emission at (λ_{em}=339 nm with excitation wavelength at (λ_{ex}=265 nm, whereas, CT-DNA didn't exhibit fluorescence by its own. A decrease in the fluorescence intensity of abiraterone was observed with addition of CT-DNA to abiraterone. The fluorescence intensity decreased further on gradual increase in the CT-DNA concentration (0-50 μM) with a fixed concentration of abiraterone (50 μM). The abiraterone and

CT-DNA fluorescence spectra at 298 K are given in Figure 3. Thus and interaction between CT-DNA and abiraterone was suggested. The inner filter effects were eliminated and the fluorescence intensity was corrected [19].

$$F_{cor} = F_{obs} \times 10^{(A_1+A_2)/2}$$

Where, F_{cor} is corrected and F_{obs} is observed fluorescence intensity; A_1 and A_2 are the respective absorbance at excitation and emission wavelengths.

Quenching constant and quenching mechanism

The quenching mechanisms involved in the biomolecules and ligands can either be static or dynamic quenching and are distinguished from one another based on their behavior at different temperatures. Diffusion is the basis of dynamic quenching, higher diffusion and strong collision quenching occurs at higher temperature. The fluorophore interacts with the quencher and forms a non-fluorescent complex amongst themselves in case of static quenching. The complex formed is relatively unstable as the temperature increases in case of static quenching [20]. The quenching of fluorescence was evaluated by the Stern-Volmer equation [21] as follows:

$$\frac{F_0}{F} = 1 + K_q \tau_0 [Q] = 1 + K_{sv}[Q]$$

where F_0 and F represent fluorescence intensity of fluorophore and with quencher, respectively; k_q is bimolecular quenching constant; τ_0 is the lifetime of the fluorophore without quencher; [Q] is the concentration of the quencher; and K_{SV} is the Stern–Volmer quenching constant [20]. The Ksv at three different temperatures of (298, 303 and 310 K) were calculated and are presented in Figure 4A, with the K_{sv} values given in Table 1. An increase in the K_{sv} values was observed as the temperature increased. However an increase the absorbance spectrum of abiraterone and CT-

DNA was observed upon increasing the concentration of CT-DNA suggests complex formation between the two.. Further, the quenching constant values obtained (Table 1) were higher than the maximum scattering collision quenching constant 2.0×10^{10} L mol^{-1} s^{-1}. [22-25]. Thus, it was inferred that static quenching occured in abiraterone -CT-DNA complex.

Binding constant and binding sites

The binding constant "K_b" was obtained from double logarithmic regression curve. It also provided information regarding the number of binding sites "n" [25-28]. From the linear regression curve of log $(F_0-F)/F$ *vs* log [Q] (Figure 4B) the "Kb" and "n" values were determined [13, 22, 23]:.

$$\log \frac{(F_0 - F)}{F} = \log K_b + n \log[\mathrm{Q}]$$

The K_b and n for the abiraterone-CT-DNA systems are given in Table 2. The value (n≈1) at all the studied temperatures infer that abiraterone and CT-DNA interacted in a molar ratio of 1:1. A decreased binding constants at high temperatures suggested abiraterone's dissociation from abiraterone-CT-DNA complex. In general terms a binding constant values in the range 10^6 to 10^8 M^{-1} suggested a strong binding affinity [29, 30]. The binding constant values between abiraterone and CT-DNA (Table 2) indicate a relatively strong binding interaction.

Binding mode and interaction forces

The non-covalent interactions that could be involved in the binding of ligands and bio-macromolecules are hydrogen bonds, van der Waals forces, and hydrophobic and electrostatic interaction [31]. The types of non–covalent interactions involved can be identified with the thermodynamic parameters such as enthalpy change (ΔH°) and entropy change (ΔS°). Hence to

evaluate binding mode and interactions the thermodynamic parameters were calculated by Van't Hoff equation:

$$\Delta G^0 = \Delta H^0 - T\Delta S^0 = -RT\ln \mathrm{K}_b$$

where R is the gas constant, T is the experimental temperature, and ΔG° is free energy change. A plot of *ln* K_b against 1/T was explored. The intercept and the slope of the plot are used to calculate ΔH° and ΔS° (Figure 4C) and the values are given in Table 2. The results suggested that hydrogen bonds contribute in the interaction between abiraterone and CT-DNA. [8, 22]. Negative ΔG° indicated spontaneous interaction between CT-DNA and abiraterone. The results are in concurrence with docking studies since the free binding energy at 298K was -34.9 kJ mol^{-1}) and the predicted energy from molecular docking was ≈ −29.65 kJ mol^{-1}. The difference in the theoretical and the experimental results can be attributed to variation in the solution environment for experimental analysis and space model for docking analysis [32].

Ethidium Bromide (EB) competitive experiment

Ethidium bromide (EB, 3,8-diamino-5-ethyl-6-phenyl-phenanthridinium bromide) is an intercalating agent in the DNA binding [10, 33] and therefore, was used to investigate and ascertain if the intercalative mode of binding was involved in the interaction. On interaction with CT-DNA, EB gives an intense emission whereas, no noticeable emission is observed with EB alone. The emission spectra for EB –CT-DNA were recoded both with and without abiraterone at 500-700 nm (λex = 524 nm nm). However, no noticeable change was observed in the emission spectrum of EB-CT-DNA on addition of abiraterone (Figure 5). EB was not displaced from its site of binding on CT-DNA by abiraterone as no change in the emission of EB-CT-DNA was observed suggesting non-intercalative binding of abiraterone and CT-DNA.

Iodide quenching studies

Binding interaction between CT-DNA and abiraterone were further elucidated with iodide quenching studies. Potassium iodide (KI) was used as quencher for abiraterone and abiraterone CT-DNA. In case of intercalative interaction between ligand and CT-DNA the ligand is protected by the double stranded CT-DNA from the quenching effect of ionic quencher whereas, in case of groove binding between ligand and CT-DNA the quenching should occur readily as the ligand is not protected from the effect of anionic quencher[34]. The quenching constants (Ksv) for abiraterone and abiraterone- CT-DNA with KI were calculated using Stern-Volmer equation Figure 6. The Ksv obtained for abiraterone-KI was similar to that for abiraterone-CT-DNA-KI demonstrating no protection by CT-DNA against quenching effect of KI. Thus, suggesting involvement of groove binding between abiraterone and CT-DNA [13].

Effect of Ionic Strength

The ionic strength studies were used to rule out the electrostatic binding mode between Abiraterone and CT-DNA. Sodium chloride (NaCl) is generally used for this purpose as it's addition has minimal effect on the fluorescence intensity of the small drug molecule. The negative charge of DNA phosphate backbone is neutralized by the sodium (Na^+), thus, decreasing the electrostatic repulsion amid weakening of surface-binding interactions. Also, the addition of Na^+ leads to decreased electrostatic attraction amid the DNA surface and the small drug molecule. In electrostatic binding, the binding occurs outside the groove and addition of NaCl results in reduced quenching of FI [12]. In the current study no change in the fluorescence intensity of abiraterone-CT-DNA was observed in presence of NaCl. Thus, ruling out the involvement of electrostatic binding mechanism between CT-DNA and abiraterone.

Molecular modeling

Molecular docking serves as an instrumental tool in studying ligand and macromolecular interactions [13, 35]. Molecular docking using MOE for abiraterone and CT-DNA was executed to attain an understanding in terms of the binding site and binding location for abiraterone in the CT-DNA. The model which showed the lowest docking energy was taken for the docking. The docking results revealed that the abiraterone interacts with the CT-DNA via minor groove binding. (Figure 7A), also, the interaction was non-covalent in nature. These results are in agreement to the values obtained experimentally. The binding energy for abiraterone and DNA was found to be -7.088 kcal mol^{-1} with the docking analysis and experimentally it was found to be -8.34 kcal mol^{-1}. Further, a hydrogen bond was also found between 3-N of abiraterone and 2-N of DG22 of chain B of DNA (Figure 7B).

Conclusions

The interaction between abiraterone and CT-DNA indicates the involvement of static quenching. Also the minor groove of CT-DNA was found to interact with Abiraterone by spontaneous hydrogen bonding with no other electrostatic interactions being involved in binding mechanism.

Acknowledgments

The authors would like to extend their sincere appreciation to the Deanship of Scientific Research, King Saud University, for funding the research group No. RG-1438-042.

References

1. Osborne, S.E. and A.D. Ellington, *Nucleic acid selection and the challenge of combinatorial chemistry.* Chemical Reviews, 1997. **97**(2): p. 349-370.
2. Sonpavde, G., et al., *The role of abiraterone acetate in the management of prostate cancer: a critical analysis of the literature.* Eur Urol, 2011. **60**(2): p. 270-278.
3. Schuster, I. and R. Bernhardt, *Inhibition of cytochromes p450: existing and new promising therapeutic targets.* Drug Metab Rev, 2007. **39**(2-3): p. 481-499.
4. Wani, T.A., *Highly sensitive ultra-performance liquid chromatography–tandem mass spectrometry method for the determination of abiraterone in human plasma.* Analytical Methods, 2013. **5**(15): p. 3693-3699.
5. Sonpavde, G., et al., *The role of abiraterone acetate in the management of prostate cancer: a critical analysis of the literature.* Eur Urol, 2011. **60**(2): p. 270-8.
6. Barrie, S., et al., *Pharmacology of novel steroidal inhibitors of cytochrome P45017α (17α-hydroxylase/C17–20 lyase).* J Steroid Biochem Mol Biol, 1994. **50**(5-6): p. 267-273.
7. Pezaro, C.J., D. Mukherji, and J.S. De Bono, *Abiraterone acetate: redefining hormone treatment for advanced prostate cancer.* Drug Discov Today, 2012. **17**(5-6): p. 221-226.
8. Mukherjee, A. and B. Singh, *Binding interaction of pharmaceutical drug captopril with calf thymus DNA: a multispectroscopic and molecular docking study.* Journal of Luminescence, 2017. **190**: p. 319-327.
9. Ikhlas, S. and M. Ahmad, *Binding studies of guggulsterone-E to calf thymus DNA by multi-spectroscopic, calorimetric and molecular docking studies.* Spectrochimica Acta Part A: Molecular and Biomolecular Spectroscopy, 2018. **190**: p. 402-408.
10. Rahman, Y., et al., *Unravelling the interaction of pirenzepine, a gastrointestinal disorder drug, with calf thymus DNA: An in vitro and molecular modelling study.* Arch Biochem Biophys, 2017. **625**: p. 1-12.
11. Wani, T.A., et al., *Evaluation of competitive binding interaction of neratinib and tamoxifen to serum albumin in multidrug therapy.* Spectrochimica Acta Part A: Molecular and Biomolecular Spectroscopy, 2019: p. 117691.
12. Rehman, S.U., et al., *Interaction of 6 mercaptopurine with calf thymus DNA–deciphering the binding mode and photoinduced DNA damage.* PLoS One, 2014. **9**(4): p. e93913.
13. Al Qumaizi, K.I., et al., *Study on the interaction of antidiabetic drug Pioglitazone with calf thymus DNA using spectroscopic techniques.* Journal of Molecular Recognition, 2018. **31**(11): p. e2735.
14. Sadeghi, M., et al., *Binding studies of the anti-retroviral drug, efavirenz to calf thymus DNA using spectroscopic and voltammetric techniques.* Luminescence, 2016. **31**(1): p. 108-117.

15. Zhang, L.Z. and G.-Q. Tang, *The binding properties of photosensitizer methylene blue to herring sperm DNA: a spectroscopic study.* Journal of Photochemistry and Photobiology B: Biology, 2004. **74**(2-3): p. 119-125.
16. Ahmad, I., A. Ahmad, and M. Ahmad, *Binding properties of pendimethalin herbicide to DNA: multispectroscopic and molecular docking approaches.* Physical Chemistry Chemical Physics, 2016. **18**(9): p. 6476-6485.
17. Shahabadi, N. and S. Hadidi, *Spectroscopic studies on the interaction of calf thymus DNA with the drug levetiracetam.* Spectrochimica Acta Part A: Molecular and Biomolecular Spectroscopy, 2012. **96**: p. 278-283.
18. Long, E.C. and J.K. Barton, *On demonstrating DNA intercalation.* Accounts of Chemical Research, 1990. **23**(9): p. 271-273.
19. Al-Mehizia, A.A., et al., *Evaluation of Biophysical Interaction between Newly Synthesized Pyrazoline Pyridazine Derivative and Bovine Serum Albumin by Spectroscopic and Molecular Docking Studies.* Journal of Spectroscopy, 2019.
20. Lakowicz, J.R., *Principles of fluorescence spectroscopy*. 2013: Springer Science & Business Media.
21. Husain, M.A., et al., *Elucidating the interaction of sulindac with calf thymus DNA: biophysical and in silico molecular modelling approach.* New Journal of Chemistry, 2017. **41**(24): p. 14924-14935.
22. Wani, T.A., et al., *Study of interactions of an anticancer drug neratinib with bovine serum albumin: Spectroscopic and molecular docking approach.* Frontiers in Chemistry, 2018. **6**: p. 47.
23. Wani, T.A., et al., *Study of the interactions of bovine serum albumin with the new anti-inflammatory agent 4-(1, 3-Dioxo-1, 3-dihydro-2H-isoindol-2-yl)-N′-[(4-ethoxy-phenyl) methylidene] benzohydrazide using a multi-spectroscopic approach and molecular docking.* Molecules, 2017. **22**(8): p. 1258.
24. Chamani, J. and M. Heshmati, *Mechanism for stabilization of the molten globule state of papain by sodium n-alkyl sulfates: spectroscopic and calorimetric approaches.* Journal of colloid and interface science, 2008. **322**(1): p. 119-127.
25. Abdelhameed, A.S., et al., *Molecular interactions ofAL3818 (anlotinib) to human serum albumin as revealed by spectroscopic and molecular docking studies.* Journal of Molecular Liquids, 2019. **273**: p. 259-265.
26. Wani, T.A., et al., *spectroscopic and molecular modeling studies of binding interaction between bovine serum albumin and roflumilast.* Drug design, development and therapy, 2018. **12**: p. 2627.
27. Wani, T.A., et al., *Spectrophotometric and molecular modelling studies on in vitro interaction of tyrosine kinase inhibitor linifanib with bovine serum albumin.* PLoS One, 2017. **12**(4): p. e0176015.
28. Alanazi, M.M., et al., *Mechanistic interaction study of 5, 6-Dichloro-2-[2-(pyridin-2-yl) ethyl] isoindoline-1, 3-dione with bovine serum albumin by spectroscopic and molecular docking approaches.* Saudi Pharmaceutical Journal, 2018.
29. Zhang, J., et al., *Comparative studies on the interaction of genistein, 8-chlorogenistein, and 3′, 8-dichlorogenistein with bovine serum albumin.* J Agric Food Chem, 2011. **59**(13): p. 7506-7513.
30. Zhang, S., et al., *Capecitabine as a minor groove binder of DNA: molecular docking, molecular dynamics, and multi-spectroscopic studies.* Journal of Biomolecular Structure and Dynamics, 2019. **37**(6): p. 1451-1463.
31. Silva, M.M., et al., *Interaction between bioactive compound 11a-N-tosyl-5-deoxi-pterocarpan (LQB-223) and Calf thymus DNA: Spectroscopic approach, electrophoresis and theoretical studies.* International Journal of Biological Macromolecules, 2017. **96**: p. 223-233.
32. Shakibapour, N., et al., *Multi-spectroscopic and molecular modeling studies to reveal the interaction between propyl acridone and calf thymus DNA in the presence of histone H1: Binary*

and ternary approaches. Journal of Biomolecular Structure and Dynamics, 2019. **37**(2): p. 359-371.

33. Pulimamidi, R.R., et al., *Picolinic acid based Cu (II) complexes with heterocyclic bases–crystal structure, DNA binding and cleavage studies.* European journal of medicinal chemistry, 2014. **79**: p. 117-127.
34. Rehman, S.U., et al., *Studying non-covalent drug–DNA interactions.* Arch Biochem Biophys, 2015. **576**: p. 49-60.
35. Bera, R., et al., *Studies on the interaction of isoxazolcurcumin with calf thymus DNA.* International Journal of Biological Macromolecules, 2008. **42**(1): p. 14-21.

List of Figures:

Figure 1: Chemical structure of abiraterone.

Figure 2: Abiraterone UV-absorption spectra in presence and absence of CT-DNA.

Figure 3: Abiraterone fluorescence spectra in absence and presence of different concentrations of CT-DNA at 298 K.

Figure 4: [A]: Abiraterone Stern–Volmer plot for its quenching by CT-DNA (298/303/310) K; [B]: The plot of log [(F_0- F)/F] versus log[Q] for quenching process of abiraterone with CT-DNA at 298/303/310 K; [C]: Van't Hoff plots for binding interaction of abiraterone and CT-DNA

Figure 5: Fluorescence spectra of CT-DNA and EB (intercalator) complex in presence of varying concentrations of abiraterone (0-50 μM).

Figure 6: Stern-Volmer plot for fluorescence quenching of abiraterone by KI in absence and presence of CT-DNA

Figure 7: [A] Abiraterone-CT-DNA docking conformation with lowest energy. [B] Abiraterone surrounded by DNA bases

Table 1: The Stern-Volmer quenching constants K_{SV} and the quenching rate constants for abiraterone -CT-DNA interaction

T(K)	R	K_{sv} (L mol^{-1})	K_q (L $mol^{-1}s^{-1}$)
298	0.9939	1.79×10^4	1.79×10^{12}
303	0.9948	2.00×10^4	2.00×10^{12}
310	0.9936	2.04×10^4	2.04×10^{12}

.

Table 2: Binding parameters and thermodynamic parameters of abiraterone-CT-DNA.

T(K)	R	K_b (L mol^{-1})	n	ΔG (kJ mol^{-1})	ΔH (kJ mol^{-1})	ΔS (J $mol^{-1}K^{-1}$
298	0.9976	1.35×10^6	1.44	-34.93	-82.8	-161
303	0.9983	0.74×10^6	1.37	-34.13		
310	0.9986	0.36×10^6	1.30	-33.00		

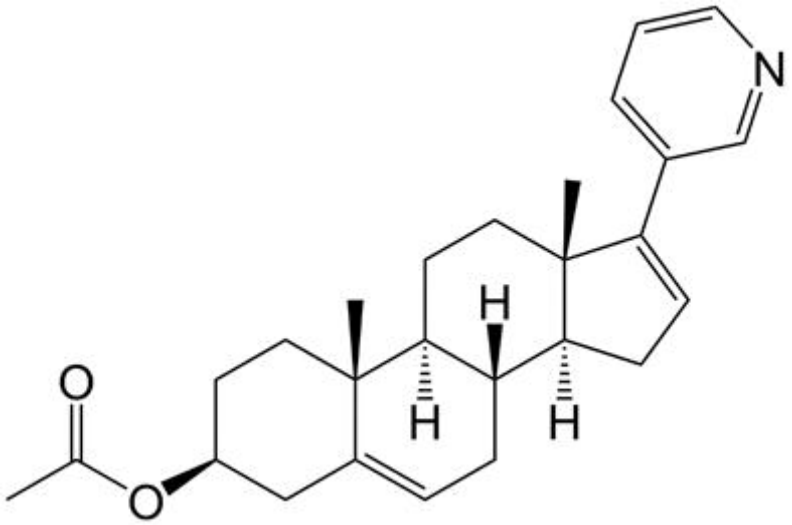
N
H
H
H
O
O

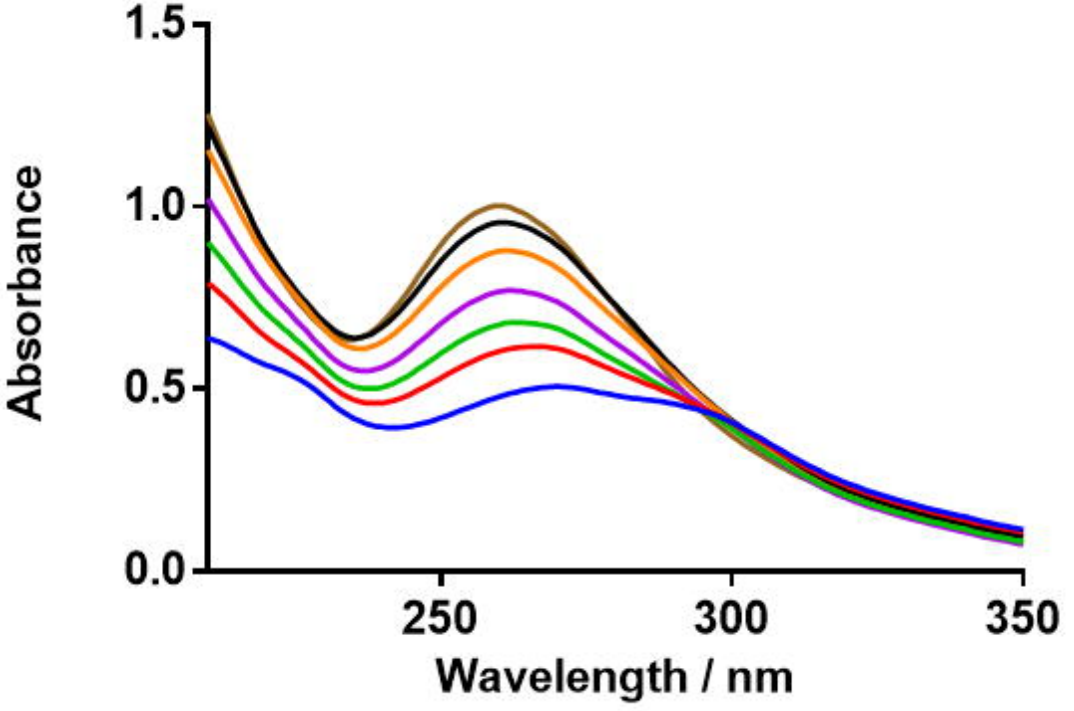
1.5
1.0
0.5
0.0
Absorbance
250
300
350
Wavelength / nm

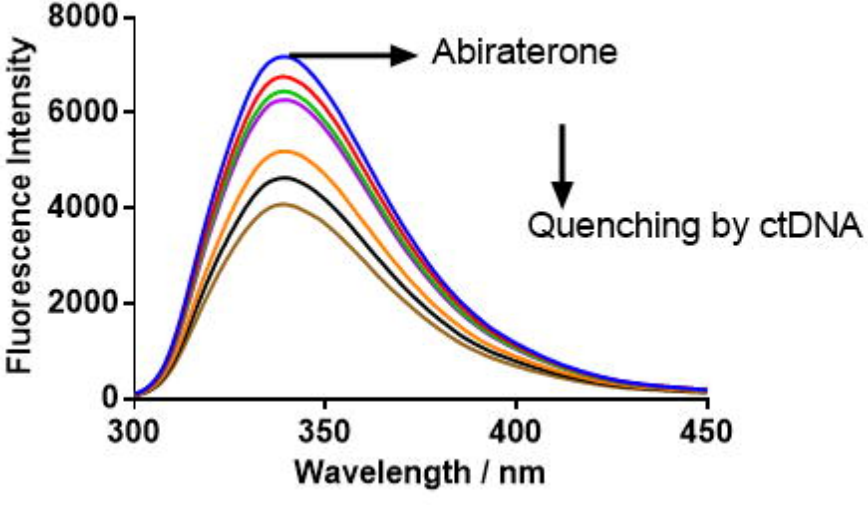
8000
6000
4000
2000
0
Fluorescence Intensity
300
350
400
450
Wavelength / nm
Abiraterone
Quenching by ctDNA

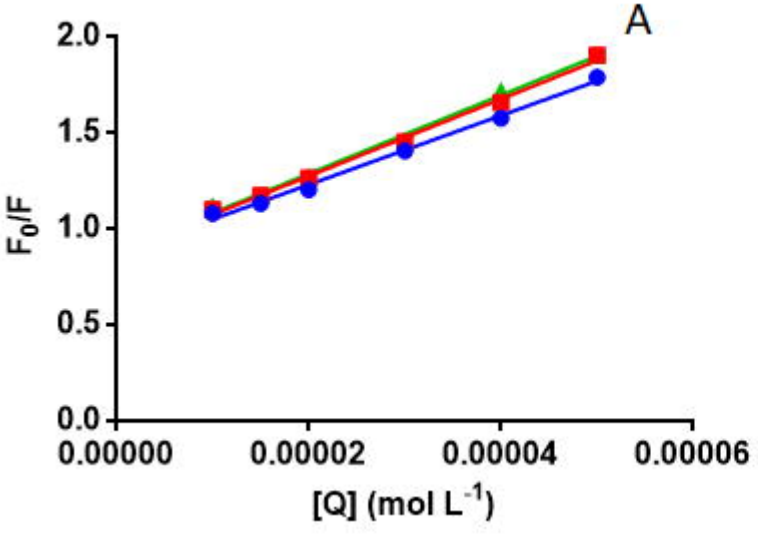
A
2.0
1.5
1.0
0.5
0.0
F_0/F
0.00000
0.00002
0.00004
0.00006
[Q] (mol L^{-1})

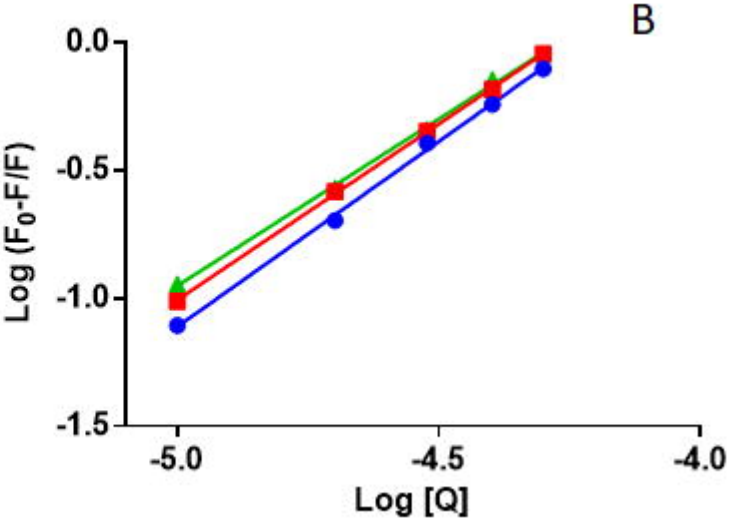
B
0.0
-0.5
-1.0
-1.5
Log (F_0-F/F)
-5.0
-4.5
-4.0
Log [Q]

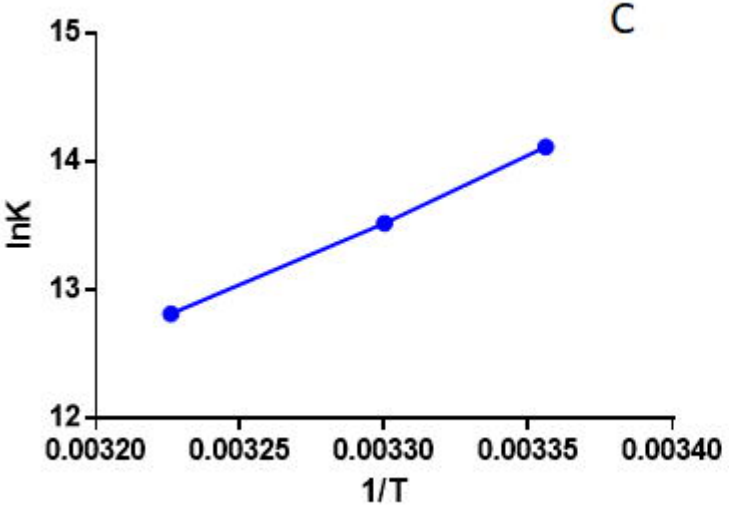
C
15
14
13
12
lnK
0.00320
0.00325
0.00330
0.00335
0.00340
1/T

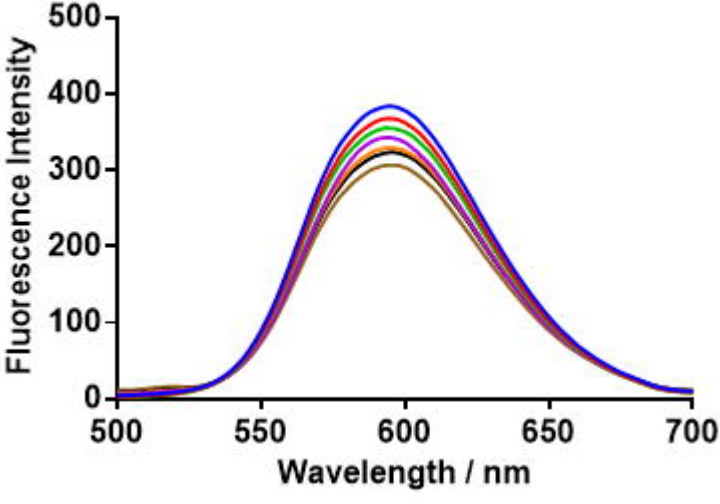
Fluorescence Intensity
500
400
300
200
100
0
500
550
600
650
700
Wavelength / nm

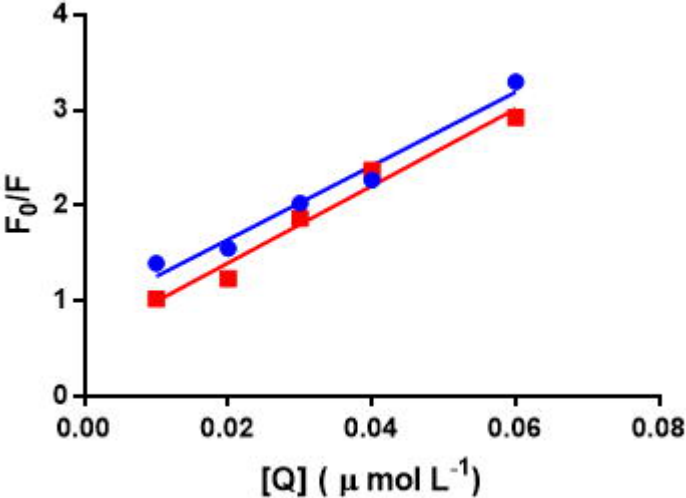
4
3
2
1
0
F_0/F
0.00
0.02
0.04
0.06
0.08
[Q] (μ mol L^{-1})

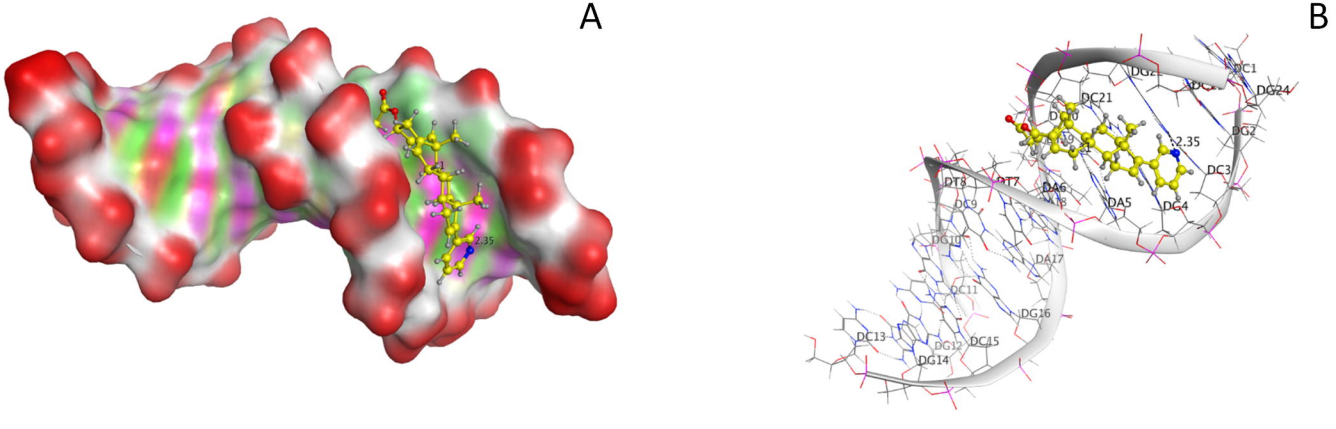
A
2.35
B
DC1
DG24
DC21
DG2
2.35
DC3
DT8
DT7
DA6
DA5
DG4
DC9
DG10
DA17
DC11
DG16
DC13
DG12
DC15
DG14